IEEE Access
Multidisciplinary | Rapid Review | Open Access Journal

Received September 9, 2017, accepted October 3, 2017, date of publication October 17, 2017,
date of current version November 28, 2017.

Digital Object Identifier 10.1109/ACCESS.2017.2762726

Polarization Filtering Based Physical-Layer Secure Transmission Scheme for Dual-Polarized Satellite Communication

ZHANGKAI LUO, HUALI WANG, (Member, IEEE), AND KAIJIE ZHOU
College of Communications Engineering, PLA Army Engineering University, Nanjing 210007, China
Corresponding author: Zhangkai Luo (luo_zhangkai@126.com)

ABSTRACT In this paper, we propose a polarization filtering-based transmission scheme to enhance the physical layer security in the dual-polarized satellite communication. To prevent eavesdropping, this paper first divides the information sequence into two parts and modulates them independently. Subsequently, a pair of dual polarization states (PSs) is selected to carry the two modulated signals based on the designed selection rule. Last but not least, two polarized signals are added up and transmitted by the orthogonally dual-polarized antenna. Based on the assumption that the selection rule of the dual polarization states is synchronous among the legitimate users, the legitimate users can separate the two polarized signals by polarization filtering (PF). After that, the polarization match is performed to the two polarized signals, respectively. Then according to the demodulation rule, the information can be recovered. However, the eavesdropper does not know the PS selection rule and could not separate the two signals. Therefore, it is impossible for the eavesdropper to recover any useful information so that the security can be enhanced. In addition, the PSs of the signals will be changed due to the polarization dependent loss effect of the satellite channel, which leads to the PF performance degradation. To tackle this problem, a zero-forcing pre-filter is utilized at the receiver side. Finally, the security performance is validated by the theoretical analysis and simulation results in the dual-polarized satellite systems.

INDEX TERMS Physical-layer secure transmission, polarization filtering, dual-polarized satellite communication.

I. INTRODUCTION

Currently, the throughput of satellite systems should be increased in order to meet the ever-increasing data demands. Furthermore, recent works have proved that multiple-input multiple-output (MIMO) is a promising way to increase the spectral efficiency by utilizing multiple antennas at both transmitters and receivers [1], [2]. Nonetheless, the MIMO technique applied in satellite communications is different from the terrestrial one, where the transmitter can obtain the channel state information (CSI) via the training sequences sent by users [3], while in satellite communications, it is difficult to update the CSI in time due to the long distance of communication. By the time the satellite receives the feedback parameters, the CSI may have been changed. Therefore, the transmission techniques which do not require CSI have grown increasingly popular.

Furthermore, satellite scenarios make the spatial components become correlate at the receiver side due to the Line of Sight (LOS). Without sufficient scatters, the receiver can only discover a signal transmission path due to the insufficient sensitivity to distinguish the different spatial signatures. Thus, the MIMO gains are hardly available [4]. Conversely, The co-located orthogonally dual-polarized antenna (ODPA) has become a low cost and space effective configuration and the usage of dual-polarized antenna in the satellite communication has been increasingly motivated by the new possible applications, together with the newest standards, including dual-polarized MIMO [5], [6]. By utilizing the ODPA, the capacity of the satellite system can be improved since polarization provides the additional degrees of freedom for information transmission [7]. In addition, the amplitude ratio and phase difference between the two orthogonally polarized branch signals can be utilized to deliver the polarization domain information. Thus, a lot of advanced techniques can be designed, such as the polarization-based modulation techniques [3], [8], [9], the polarization multiple

access technique [6], the polarization-based signal sensing technique [10], the multidimensional constellation design technique [11] and the polarization filtering technique [12].

On the other hand, security is a fundamental problem in the dual-polarized satellite communication due to the open nature of the wireless medium and its wide beam coverage, which make it difficult to shield the transmitted signals from the unintended recipients [13]. Transmission security traditionally depends on cryptographic techniques in the link and network layer [14]. The challenges (and vulnerabilities) associated with the key distribution and management, however, make cryptography a less ideal solution. New researches on physical layer security have pointed out that a positive secret rate can be guaranteed when the legitimate users have a higher signal-to-noise ratio (SNR) than the eavesdroppers based on the information theory [15]. Nonetheless, it is not always the case in the dual-polarized satellite communication, since there is no extra degree of freedom for beamforming or designing artificial noise in order to improve the secret rate [16]. To enhance the security performance, in [17], a method based on polarization modulation and weighted fractional Fourier transform (PM-WFRFT) is proposed, where the confidential message is concealed in the polarization state (PS) of the carrier. By randomly changing the WFRFT order, the signals are difficult to be detected and the constellation is distorted at the eavesdropper side. In [18], a fast dual polarization hopping (FDPH) approach is proposed, in which two PSs are used to carry the same signals. By randomly selecting the PSs, the signals vary randomly at the receiver side. Based on the assumption that the polarization hopping pattern is synchronous among the legitimate users, the eavesdropper cannot recover any useful information. However, since one of the polarized signal is useless for the legitimate users, about half of the transmitting power is wasted.

In this paper, we put forward a polarization filtering based transmission scheme to enhance the physical layer security (PF-PHY) in dual-polarized satellite communications. Firstly, the information sequence is divided into two parts, which are modulated independently with modulation techniques like Phase Shift Keying (PSK), Pulse Amplitude Modulation (PAM), and Quadrature Amplitude Modulation (QAM). Subsequently, so as to prevent eavesdropping, a pair of dual polarization states are selected based on the designed selection rule to carry the two modulated signals, respectively. Finally, two modulated signals are added up and transmitted by the ODPA. For the legitimate user, with the selection rule, two signals can be separated completely by the method of polarization filtering (PF). Subsequently, according to the demodulation rule, the information can be recovered. For the eavesdropper, it is almost impossible to separate the two signals without knowing the PS selection rule. Thereby, the received signals are random complex numbers which cannot be demodulated, thus the transmission security is enhanced. In addition, the PSs of the received signal are always different from those of the transmit signals due to the polarization dependent loss effect (PDL), which is ascribed to the non-ideal cross-polarization discrimination (XPD) of the receiver antenna as well as the complex electromagnetic environment. To address this problem, the zero-forcing pre-filter (ZFPF) is used at the receiver side to process the received signals before PF. More specifically, main contributions are summarized as below:

1. In the PF-PHY scheme, two signals with different PSs are utilized to carry the information, which is different from the FDPH method in [18], where the same signal with different PSs is used to carry the information. With the same modulation technique and transmitting power, the transmission efficiency of PF-PHY is about twice than that of FDPH.

2. The PSs of two modulated signals are controlled by the designed selection rule, which is synchronous among the legitimate users. Thereby, the signals can be separated by the legitimate users with the PF method. In the PF-PHY scheme, modulation techniques like PSK, QAM, and PAM can be directly used to modulate the signals, while PSK cannot be directly used in the FDPH system. The secure performance is evaluated in terms of the bit error rate (BER).

3. In the PF-PHY scheme, the ZFPF method is utilized to solve the PDL effect, which is different from the pre-compensation (PC) method in FDPH. By utilizing the ZFPF method, we just have to calculate the ZFPF matrix during every channel estimation interval. However, if the PC method is used, it is necessary to calculate the pre-compensation matrix at the symbol rate, which needs more calculations. In addition, in the ZFPF method, CSI is estimated at the receiver side, which is more practical in satellite scenarios.

The rest of this paper is organized as follows. In Section II, the system model will be introduced, and then the polarization dependent loss of the satellite channel and the blind signal demodulation method will be described, respectively. In Section III, the principle of the PF-PHY scheme will be described in detail. Simulation results will be presented in Section IV. Finally, Section V will provide a conclusion of this paper.

Notations: The superscript T and H are used to denote the transpose and the Hermitian transpose of a vector or matrix. Vectors and matrices are represented by bold lowercase or uppercase. Eq. (a) denotes the equation (a).

II. SYSTEM MODEL

Assuming a satellite scenario with three participants: a transmitter Alice, a legitimate receiver Bob and an eavesdropper Eve as shown in Fig. 1. In order to transmit or receive the polarized signals, all of them are equipped with a dual-polarized antenna. As the signals are broadcast from Alice to the two receivers, the eavesdropper can recover the same information as Bob, thus the information is eavesdropped. To prevent eavesdropping, we proposed a secure transmission method based on polarization filtering in this study.

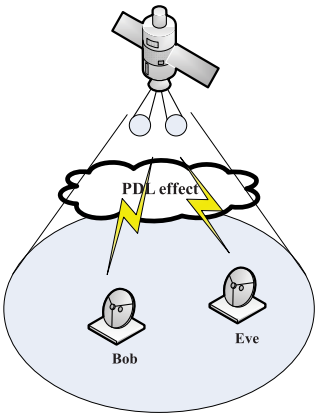

FIGURE 1. System model.

A. SIGNAL MODEL AND POLARIZATION DEPENDENT LOSS OF THE SATELLITE CHANNEL

The polarized signal represented by Jones vector can be written as [19]

$$\mathbf{s}(t) = \begin{bmatrix} \cos\gamma \\ \sin\gamma e^{j\eta} \end{bmatrix} A_k e^{j(w_c t+\varphi_k)}, \tag{1}$$

where $\gamma \in \left[0, \frac{\pi}{2}\right]$ is the amplitude relationship (or polarized angle) between the orthogonal dual-polarized components; $\eta \in [0, 2\pi]$ denotes the difference of them in phase; w_c is the carrier frequency; $A_k e^{j\varphi_k}$ denotes the amplitude-phase modulation signal and the polarization state (PS) is defined as $\mathbf{P}: (\gamma, \eta)$.

At the receiver side, the received signal can be represented as

$$\mathbf{y}(t) = \begin{bmatrix} y_1(t) \\ y_2(t) \end{bmatrix} = \mathbf{H}\mathbf{s}(t) + \mathbf{n}, \tag{2}$$

where $\mathbf{n}$ is the noise vector with the probability density function (PDF) as CN $\left(0, \sigma^2\mathbf{E}_{2\times 2}\right)$; $\mathbf{E}$ denotes the identity matrix; $\mathbf{H}$ denotes the satellite channel impulse response matrix, which can be further written as

$$\mathbf{H} = \begin{bmatrix} h_{11} & h_{12} \\ h_{21} & h_{22} \end{bmatrix} = \sqrt{\Upsilon}\mathbf{U}\mathbf{\Sigma}\mathbf{V} = \sqrt{\Upsilon}\mathbf{U}\begin{bmatrix} \sqrt{\lambda_1} & 0 \\ 0 & \sqrt{\lambda_2} \end{bmatrix}\mathbf{V}, \tag{3}$$

where Υ is the power fading of the non-polarized channel and $\sqrt{\lambda_i}, i = 1, 2$ denote eigenvalues; $\mathbf{U}$, $\mathbf{V}$ are unitary matrixes. Then, Eq. (2) can be further written as

$$\begin{aligned}
\mathbf{H}\mathbf{s}(t) &= \sqrt{\Upsilon}\mathbf{U}\begin{bmatrix} \sqrt{\lambda_1} & 0 \\ 0 & \sqrt{\lambda_2} \end{bmatrix}\mathbf{V}\underbrace{\begin{bmatrix} \cos\gamma \\ \sin\gamma e^{j\eta} \end{bmatrix}}_{\mathbf{P}_j} A_k e^{j(w_c t+\varphi_k)} \\
&= \sqrt{\Upsilon}\mathbf{U}\begin{bmatrix} \sqrt{\lambda_1} & 0 \\ 0 & \sqrt{\lambda_2} \end{bmatrix}\underbrace{\begin{bmatrix} \cos\gamma \\ \sin\gamma e^{j\bar{\eta}} \end{bmatrix}}_{\mathbf{P}_m} A_k e^{j(w_c t+\varphi_k)} \\
&= \sqrt{\Upsilon}\mathbf{U}\begin{bmatrix} \sqrt{\lambda_1}\cos\gamma \\ \sqrt{\lambda_2}\sin\gamma e^{j\bar{\eta}} \end{bmatrix} A_k e^{j(w_c t+\varphi_k)} \\
&= p\mathbf{U}\underbrace{\begin{bmatrix} \cos\tilde{\gamma} \\ \sin\tilde{\gamma} e^{j\bar{\eta}} \end{bmatrix}}_{\mathbf{P}_g} A_k e^{j(w_c t+\varphi_k)} \\
&= p\underbrace{\begin{bmatrix} \cos\tilde{\gamma} \\ \sin\tilde{\gamma} e^{j\bar{\eta}} \end{bmatrix}}_{\mathbf{P}_f} A_k e^{j(w_c t+\varphi_k)},
\end{aligned} \tag{4}$$

where $\tilde{\gamma} = \arctan\left(\sqrt{\frac{\lambda_2}{\lambda_1}}\tan\gamma\right)$ and p is the normalization power factor as

$$p = \sqrt{\Upsilon\left(\left(\sqrt{\lambda_1}\cos\gamma\right)^2 + \left(\sqrt{\lambda_2}\sin\gamma\right)^2\right)}. \tag{5}$$

For a better understanding of the PDL effect, we utilize a constellation point $\mathbf{P}_j$ to illustrate the polarization transformation in Eq. (4). As shown in Fig. 2 on the Poincare ball [20], where 2γ and η denote the length of the arc from $\mathbf{P}_j$ to the horizontal PS $\mathbf{P}_\mathrm{H}$ and the angle between this arc and the equator respectively. Affected by $\mathbf{V}$, $\mathbf{P}_j: (\gamma, \eta)$ rotates around $\mathbf{P}_\mathrm{H}$ with the radius 2γ, which results in $\mathbf{P}_m: (\gamma, \bar{\eta})$ without changing its power. This is because $\mathbf{U}$ is a unitary matrix and it creates lossless polarization transfer. Then affected by $\mathbf{\Sigma}$, it moves toward $\mathbf{P}_\mathrm{H}$ as is shown by $\mathbf{P}_g: (\tilde{\gamma}, \bar{\eta})$ and its power changes into p. Finally, affected by $\mathbf{U}$, it rotates around $\mathbf{P}_\mathrm{H}$ with the radius $2\tilde{\gamma}$ and results in $\mathbf{P}_f: (\tilde{\gamma}, \tilde{\eta})$ without changing its power. If $\mathbf{H}$ is an ideal channel with $\lambda_1 = \lambda_2 = 1$, then $\mathbf{P}_j = \mathbf{P}_f$. Nevertheless, $\mathbf{H}$ is always non-ideal due to the below reasons:

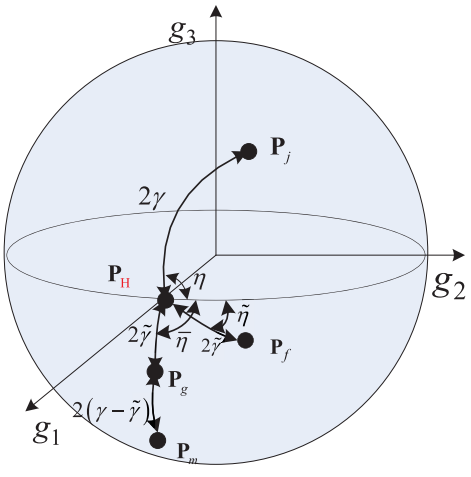

FIGURE 2. Polarization transformation on Poincare ball.

1. The cross-polarization discrimination (XPD) of the dual-polarized antenna at the receiver side is not large enough to ensure $h_{12} = h_{21} = 0$.

2. The complex electromagnetic environment, including the existing varieties of clouds, rain and small ice crystals in the air, will cause signal reflection, diffraction and diffuse scattering.

Consequently, the PSs of the received signal are always different from the transmit ones in most of the satellite scenarios.

This is the polarization dependent loss effect (PDL), which can be defined as

$$PDL = 10\log 10\left(\frac{\lambda_1}{\lambda_2}\right), \quad \lambda_1 \geq \lambda_2. \tag{6}$$

Although the PS is changed due to the PDL effect, we can still recover the information by the blind signal demodulation method, which will be described in the following part.

B. BLIND SIGNAL DEMODULATION

The block diagram of blind signal demodulation is shown in Fig. 3 Based on Eq. (2), the receivers can recover the polarization parameters $(\gamma_{\mathrm{R}}, \eta_{\mathrm{R}})$ by

$$\begin{aligned} \gamma_{\mathrm{R}} &= \arctan\left(\frac{\mathrm{abs}\left(y_2\left(t\right)\right)}{\mathrm{abs}\left(y_1\left(t\right)\right)}\right), \\ \eta_{\mathrm{R}} &= \Xi\left(y_2\left(t\right)\right) - \Xi\left(y_1\left(t\right)\right), \end{aligned} \tag{7}$$

where Ξ is the phase acquisition function. Then after the polarization match, the received signal can be represented as

$$\begin{aligned} \mathbf{y_R}\left(t\right) &= p\begin{bmatrix} \cos\gamma_{\mathrm{R}} \\ \sin\gamma_{\mathrm{R}} e^{j\eta_{\mathrm{R}}} \end{bmatrix}^{\mathrm{H}} \begin{bmatrix} \cos\tilde{\gamma} \\ \sin\tilde{\gamma} e^{j\tilde{\eta}} \end{bmatrix} A_k e^{j(w_c t+\varphi_k)} \\ &= p\left(\cos\gamma_{\mathrm{R}}\cos\tilde{\gamma} + \sin\gamma_{\mathrm{R}}\sin\tilde{\gamma} e^{j(\tilde{\eta}-\eta_{\mathrm{R}})}\right) A_k e^{j(w_c t+\varphi_k)}. \end{aligned} \tag{8}$$

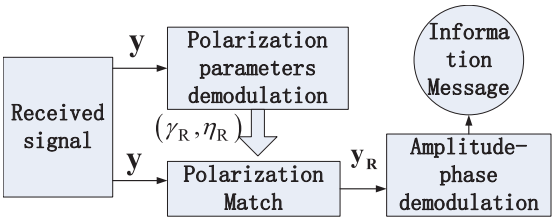

FIGURE 3. Block diagram of blind signal demodulation.

If the noise effect is ignored, according to Eq. (4) and Eq. (7), we can find $\gamma_{\mathrm{R}} = \tilde{\gamma}$, $\eta_{\mathrm{R}} = \tilde{\eta}$, then

$$\mathbf{y_R}\left(t\right) = pA_k e^{j(w_c t+\varphi_k)}. \tag{9}$$

Thus, in the satellite scenarios, it can be found that the polarization characteristics of the received signals are always different from the transmit ones due to the PDL effect. Although the polarization characteristics are changed, all the receivers can still recover the information based on the blind signal demodulation method.

III. PRINCIPLE OF THE PF-PHY SCHEME

A. TRANSMITTER MODEL

As analyzed in the last section, even the PS of the signal is randomly changed at the symbol rate, it cannot prevent eavesdropping. Thus, in this section, the information is divided into two parts and two different PSs are assigned to them. Then, both of the two parts are added up and transmitted by the dual-polarized antenna. By randomly changing the PSs at the symbol rate, the transmission security can be realized.

The block diagram of the transmitter is presented in Fig. 4. At first, the information sequence I_O is divided into I_x and I_l by the Data Rate Allocation Unit (DRAU). Subsequently, both of them are modulated by the traditional modulation (TM) techniques, which yields K symbols: x_k, l_k, $k = 1, 2, \cdots, K$. Later, K pairs of different PSs are assigned to them, respectively. Finally, the two polarized signals are added together and send to the radio frequency unit (RF). After that, the composite signal is transmitted out by the horizontally-polarized antenna (H) and vertically-polarized antenna (V).

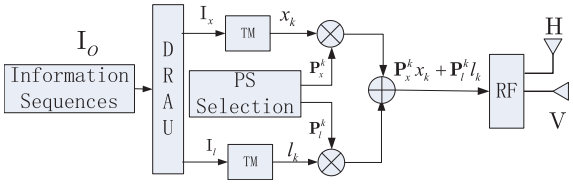

FIGURE 4. Block diagram of the transmitter.

B. POLARIZATION FILTERING AT THE RECEIVER SIDE UNDER THE IDEAL GAUSS CHANNEL

If the channel is ideal, the received signal can be represented as

$$\begin{aligned} \mathbf{y}_k\left(t\right) &= \mathbf{s}_x^k\left(t\right) + \mathbf{s}_l^k\left(t\right) + \mathbf{n} \\ &= \begin{bmatrix} \cos\gamma_x^k \\ \sin\gamma_x^k e^{j\eta_x^k} \end{bmatrix} A_x^k e^{j(w_c t+\varphi_x^k)} \\ &\quad + \begin{bmatrix} \cos\gamma_l^k \\ \sin\gamma_l^k e^{j\eta_l^k} \end{bmatrix} A_l^k e^{j(w_c t+\varphi_l^k)} + \mathbf{n}. \end{aligned} \tag{10}$$

From Eq. (10), it is found that signals cannot be directly demodulated with the usage of Eq. (7) and in order to demodulate the received signal, two polarized signals should be firstly separated. Polarization filtering (PF) is a mature technology and used to solve the problems of signal separation, which are difficult to process in the time, frequency and spatial domains [12].

To illustrate the principle of polarization filtering, we assume two Jones vectors $\mathbf{P}_x^k$: $\left(\gamma_x^k, \eta_x^k\right)$ and $\mathbf{P}_l^k$: $\left(\gamma_l^k, \eta_l^k\right)$ with different polarization parameters: $\gamma_x^k \neq \gamma_l^k$ or $\eta_x^k \neq \eta_l^k$. Then, the oblique projection operator for polarization filtering can be represented as

$$\begin{aligned} \mathbf{Q}_{\mathbf{P}_x^k|\mathbf{P}_l^k} &= \mathbf{P}_x^k\left(\left(\mathbf{P}_x^k\right)^{\mathbf{H}} P_{\mathbf{P}_l^k}^{\perp}\mathbf{P}_x^k\right)^{-1}\left(\mathbf{P}_x^k\right)^{\mathbf{H}} P_{\mathbf{P}_l^k}^{\perp}, \\ \mathbf{Q}_{\mathbf{P}_l^k|\mathbf{P}_x^k} &= \mathbf{P}_l^k\left(\left(\mathbf{P}_l^k\right)^{\mathbf{H}} P_{\mathbf{P}_x^k}^{\perp}\mathbf{P}_l^k\right)^{-1}\left(\mathbf{P}_l^k\right)^{\mathbf{H}} P_{\mathbf{P}_x^k}^{\perp}, \end{aligned} \tag{11}$$

where

$$\begin{aligned} \mathbf{P}_{\mathbf{P}_l^k}^{\perp} &= \mathbf{E} - \mathbf{P}_l^k\left(\left(\mathbf{P}_l^k\right)^{\mathbf{H}}\mathbf{P}_l^k\right)^{-1}\left(\mathbf{P}_l^k\right)^{\mathbf{H}}, \\ \mathbf{P}_{\mathbf{P}_x^k}^{\perp} &= \mathbf{E} - \mathbf{P}_x^k\left(\left(\mathbf{P}_x^k\right)^{\mathbf{H}}\mathbf{P}_x^k\right)^{-1}\left(\mathbf{P}_x^k\right)^{\mathbf{H}}. \end{aligned} \tag{12}$$

where $\mathbf{E}$ denotes the identity matrix. Based on Eq. (11) and Eq. (12), the below formulas are obtained:

$$\begin{aligned} \mathbf{Q}_{\mathbf{P}_x^k|\mathbf{P}_l^k}\mathbf{P}_x^k &= \mathbf{P}_x^k, \quad \mathbf{Q}_{\mathbf{P}_x^k|\mathbf{P}_l^k}\mathbf{P}_l^k = \mathbf{0}, \\ \mathbf{Q}_{\mathbf{P}_l^k|\mathbf{P}_x^k}\mathbf{P}_l^k &= \mathbf{P}_l^k, \quad \mathbf{Q}_{\mathbf{P}_l^k|\mathbf{P}_x^k}\mathbf{P}_x^k = \mathbf{0}. \end{aligned} \tag{13}$$

Then based on Eq. (10), the below can be obtained

$$\begin{aligned} \mathbf{P}_x^k x_x^k &= \mathbf{Q}_{\mathbf{P}_x^k|\mathbf{P}_l^k}\mathbf{y}_k\ (t) \\ &= \begin{bmatrix} \cos\gamma_x^k \\ \sin\gamma_x^k e^{j\eta_x^k} \end{bmatrix} A_x^k e^{j(w_c t+\varphi_x^k)} + \mathbf{Q}_{\mathbf{P}_x^k|\mathbf{P}_l^k}\mathbf{n}, \\ \mathbf{P}_l^k x_l^k &= \mathbf{Q}_{\mathbf{P}_l^k|\mathbf{P}_x^k}\mathbf{y}_k\ (t) \\ &= \begin{bmatrix} \cos\gamma_l^k \\ \sin\gamma_l^k e^{j\eta_l^k} \end{bmatrix} A_l^k e^{j(w_c t+\varphi_l^k)} + \mathbf{Q}_{\mathbf{P}_l^k|\mathbf{P}_x^k}\mathbf{n}. \end{aligned} \tag{14}$$

From Eq. (14), it is found that two signals are separated.

C. POLARIZATION STATE SELECTION

Although two signals are separated, it is noteworthy that the noise power is changed after processed by PF, which can be denoted as (we take $\mathbf{Q}_{\mathbf{P}_x^k|\mathbf{P}_l^k}\mathbf{n}$ for an example and the analysis is the same for $\mathbf{Q}_{\mathbf{P}_l^k|\mathbf{P}_x^k}\mathbf{n}$)

$$\tilde{\sigma}^2 = \text{trace}\left(\mathbf{Q}_{\mathbf{P}_x^k|\mathbf{P}_l^k}\left(\mathbf{Q}_{\mathbf{P}_x^k|\mathbf{P}_l^k}\right)^H \sigma^2\right) = \frac{\sigma^2}{\sin^2\xi}, \tag{15}$$

where ξ is the principal angle between the subspace of $\mathbf{P}_x^k$ and $\mathbf{P}_l^k$ on the Poincare sphere [19]. As $\sin^2\xi \leq 1$, the noise is amplified by PF. Indeed, the relationship between the output SNR and the input SNR can be described as

$$\Delta = SNR_{out} - SNR_{in} = 20\log\sin(\xi). \tag{16}$$

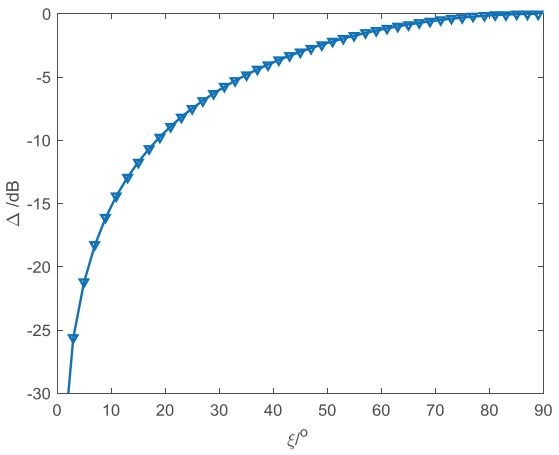

FIGURE 5. Effect of the principle angle ξ on the output SNR.

Fig. 5 shows the effect of the principle angle ξ on the output SNR. It can be found that when ξ tends to 90°, there is almost no change in SNR. Thus, Johns vectors with orthogonal polarizations are ideal choices.

As shown in Fig. 6, two points on the surface of the sphere are potential orthogonal polarization representations if the line joining them can pass through the center of the sphere, such as the pairs $(\mathbf{P}_1, \mathbf{P}_2)$, $(\mathbf{P}_3, \mathbf{P}_4)$. In this way, the noise power is not amplified. Therefore, in the PF-PHY scheme, the PSs can be generated by the following steps:

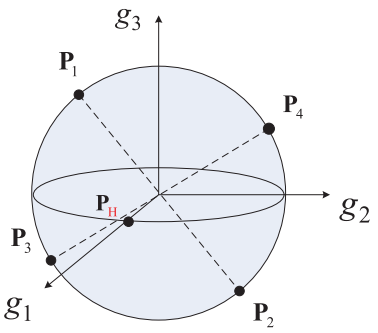

FIGURE 6. Constellations with orthogonal polarization.

1. Generate two independent pseudo-random sequences based on the method in [21], such as PN1, PN2.
2. PN1 is used to determine the polarization angle $\gamma_x^k \in \left(0, \frac{\pi}{2}\right)$ and PN2 is used to determine $\eta_x^k \in (0, 2\pi)$.
3. Once a PS $\mathbf{P}_x^k : \left(\gamma_x^k, \eta_x^k\right)$ is chosen, its orthogonal polarization state $\mathbf{P}_l^k$ can be obtained by:

$$\gamma_l^k = \frac{\pi}{2} - \gamma_x^k, \eta_l^k = \pi + \eta_x^k. \tag{17}$$

The legitimate user Bob is aware of the PS selection rule, during each symbol period, the PSs $\mathbf{P}_x^k$ and $\mathbf{P}_l^k$ are selected at the transmitter to carry the traditional modulation signals. Then, at the receiver side, the same PSs $\mathbf{P}_x^k$ and $\mathbf{P}_l^k$ can be selected to form the polarization filters to separate the two transmit signals. However, the eavesdropper does not know the rule and it is impossible to intercept and capture from the received signal. Hence, it is almost impossible to separate two signals.

D. DEPOLARIZATION ELIMINATION

Under the ideal channel condition, the polarized signals can be separated by PF. Nonetheless, the polarization characteristic of the transmit signal will be changed due to the PDL effect of the satellite channel as illustrated in section II-A. Thus, although Bob knows the PS selection rule, it is still impossible to completely separate two signals [10].

In order to solve the PDL effect, previous works mainly emphasize on the pre-compensation method based on the estimated channel state information (CSI) at the transmitter side [18], [20], [22]. For instance, for $\mathbf{P}_x^k$ (the pre-compensation matrix of $\mathbf{P}_l^k$ can be calculated in the same way by changing the polarization parameters), the pre-compensation matrix can be calculated by

$$\mathbf{\Psi}_x^k = \mathbf{V}^{\mathrm{H}} \begin{bmatrix} \frac{\sqrt{\lambda_2}}{\sqrt{\lambda_2\sin^2\gamma_x^k + \lambda_1\cos^2\gamma_x^k}} & 0 \\ 0 & \frac{\sqrt{\lambda_1}}{\sqrt{\lambda_2\sin^2\gamma_x^k + \lambda_1\cos^2\gamma_x^k}} \end{bmatrix} \mathbf{U}^{\mathrm{H}}. \tag{18}$$

According to Eq. (2), Eq. (3) and Eq. (10), the received signal can be represented as

$$\begin{aligned}\widehat{\mathbf{y}}_k(t) &= \mathbf{H}\boldsymbol{\Psi}_x^k\mathbf{s}_x^k(t) + \mathbf{H}\boldsymbol{\Psi}_l^k\mathbf{s}_l^k(t) + \mathbf{n} \\ &= p_x^k\begin{bmatrix}\cos\gamma_x^k \\ \sin\gamma_x^k e^{j\eta_x^k}\end{bmatrix}A_x^k e^{j(w_c t+\varphi_x^k)} \\ &\quad + p_l^k\begin{bmatrix}\cos\gamma_l^k \\ \sin\gamma_l^k e^{j\eta_l^k}\end{bmatrix}A_l^k e^{j(w_c t+\varphi_l^k)} + \mathbf{n}. \\ p_z^k &= \frac{\sqrt{\Upsilon\lambda_1\lambda_2}}{\sqrt{\lambda_2\sin^2\gamma_z^k + \lambda_1\cos^2\gamma_z^k}}, \quad z = x, l. \end{aligned} \tag{19}$$

Although the pre-compensation method can prevent the distortion of the PSs, it will cause power attenuation [22]. In addition, the pre-compensation matrix for both signals should be updated at the symbol rate, which requires a large amount of calculation. Moreover, it may not be the case to timely update the CSI at the transmitter side in the satellite scenarios due to the long communication distance. Thus, in the PF-PHY scheme, the CSI is estimated at the receiver side and a zero-forcing pre-filter (ZFPF) is applied before PF [23], which is equivalent to applying the filter

$$\mathbf{W} = \mathbf{G}^{-1} = \frac{\mathbf{G}^*}{\det(\mathbf{G})}, \tag{20}$$

where $\mathbf{G}$ denotes the estimated CSI and we assume $\mathbf{G} = \mathbf{H}$.

$$\mathbf{G}^* = \begin{bmatrix} h_{22} & -h_{12} \\ -h_{21} & h_{11}\end{bmatrix}. \tag{21}$$

As the channel estimation is not the main theme in our research, it is omitted here and we assume the perfect CSI at the receiver side. The signals after processing can be denoted as:

$$\begin{aligned}\bar{\mathbf{y}}_k(t) &= \mathbf{W}\mathbf{H}\mathbf{s}_x^k(t) + \mathbf{W}\mathbf{H}\mathbf{s}_l^k(t) + \mathbf{W}\mathbf{n} \\ &= \mathbf{s}_x^k(t) + \mathbf{s}_l^k(t) + \mathbf{W}\begin{bmatrix}n_1^k \\ n_2^k\end{bmatrix} \\ &= \mathbf{s}_x^k(t) + \mathbf{s}_l^k(t) + \begin{bmatrix}\hat{n}_1^k \\ \hat{n}_2^k\end{bmatrix},\end{aligned} \tag{22}$$

where $\hat{n}_1^k = \frac{h_{22}n_1^k - h_{12}n_2^k}{\det(\mathbf{H})}$, $\hat{n}_2^l = \frac{h_{11}n_2^k - h_{21}n_1^k}{\det(\mathbf{H})}$. It is easy to prove that the PDFs are [24]

$$\begin{aligned}\hat{n}_1^k &\sim \mathrm{CN}\left(0, \frac{|h_{22}|^2 + |h_{12}|^2}{\det(\mathbf{H})^2}\sigma^2\right), \\ \hat{n}_2^k &\sim \mathrm{CN}\left(0, \frac{|h_{11}|^2 + |h_{21}|^2}{\det(\mathbf{H})^2}\sigma^2\right).\end{aligned} \tag{23}$$

According to Eq. (23), it is easy to find that the noise power is amplified. Based on the ZFPF method, the depolarization effect is eliminated and we just have to update the ZFPF matrix during every channel estimation interval, instead of the symbol rate in the pre-compensation method. In addition, the CSI is estimated at the receiver side, which is more practical in satellite scenarios.

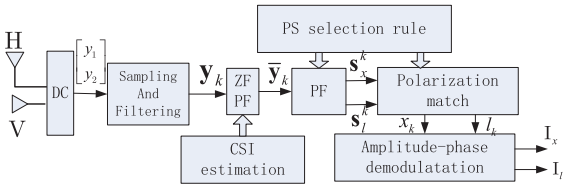

FIGURE 7. The block diagram of the receiver for Bob.

Finally, the block diagram of the receiver designed for Bob is presented in Fig. 7. After sampling and filtering, the PDL effect is firstly eliminated based on the ZFPF method. Subsequently, by utilizing the PSs of the two polarized signals, which are strictly synchronous with the transmitter, the two signals $\mathbf{s}_x(t)$, $\mathbf{s}_l(t)$ are separated. After that, the polarization match is applied to obtain the modulation signals for recovering the original input information.

E. PERFORMANCE EVALUATION

In this paper, we consider a more practical model that both the legitimate receiver Bob and the eavesdropper Eve can accurately obtain the CSI. Thus Eve can also apply the ZFPF method to eliminate the PDL effect. Then, ignore the effect of the noise, according to Eq. (17), for Eve, the received signal can be denoted as

$$\begin{aligned}\mathbf{y}_{\mathrm{E}}^k(t) &= \mathbf{s}_x^k(t) + \mathbf{s}_l^k(t) \\ &= \left(\begin{bmatrix}\cos\gamma_x^k \\ \sin\gamma_x^k e^{j\eta_x^k}\end{bmatrix}A_x^k e^{j\varphi_x^k} + \begin{bmatrix}\cos\gamma_l^k \\ \sin\gamma_l^k e^{j\eta_l^k}\end{bmatrix}A_l^k e^{j\varphi_l^k}\right)e^{jw_c t} \\ &= \begin{bmatrix}\cos\gamma_x^k \\ \sin\gamma_x^k e^{j\eta_x^k}\end{bmatrix}A_x^k e^{j(w_c t+\varphi_x^k)} \\ &\quad + \begin{bmatrix}\cos\left(\frac{\pi}{2} - \gamma_x^k\right) \\ \sin\left(\frac{\pi}{2} - \gamma_x^k\right)e^{j(\eta_x^k+\pi)}\end{bmatrix}A_l^k e^{j(w_c t+\varphi_l^k)}.\end{aligned} \tag{24}$$

As Eve does not know the PSs of the polarized signals, it is almost impossible to separate the two polarized signals. If the eavesdropper adopts the blind signal demodulation method as discussed in II-B, the polarization parameters are

$$\begin{aligned}\gamma_{\mathrm{ER}}^k &= \arctan\left(\frac{\left|A_x^k\sin\left(\gamma_x^k\right)e^{j\eta_x^k}e^{j\varphi_x^k} - A_l^k\cos\left(\gamma_x^k\right)e^{j\eta_x^k}e^{j\varphi_l^k}\right|}{\left|A_x^k\cos\left(\gamma_x^k\right)e^{j\varphi_x^k} + A_l^k e^{j\varphi_l^k}\sin\left(\gamma_x^k\right)\right|}\right), \\ \eta_{\mathrm{ER}}^k &= \Xi\left(A_x^k\sin\left(\gamma_x^k\right)e^{j\eta_x^k}e^{j\varphi_x^k} - A_l^k\cos\left(\gamma_x^k\right)e^{j\eta_x^k}e^{j\varphi_l^k}\right) \\ &\quad - \Xi\left(A_x^k\cos\left(\gamma_x^k\right)e^{j\varphi_x^k} + A_l^k e^{j\varphi_l^k}\sin\left(\gamma_x^k\right)\right).\end{aligned} \tag{25}$$

Subsequently, the blind demodulated signal can be represented as

$$\begin{aligned}y_{\mathrm{ER}}^k(t) &= \cos\gamma_{\mathrm{ER}}^k\cos\gamma_x^k A_x^k e^{j(w_c t+\varphi_x^k)} \\ &\quad + \sin\gamma_{\mathrm{ER}}^k\sin\gamma_x^k e^{j(\eta_x^k-\eta_{\mathrm{ER}}^k)}A_x^k e^{j(w_c t+\varphi_x^k)} \\ &\quad + \cos\gamma_{\mathrm{ER}}^k\sin\gamma_x^k A_l^k e^{j(w_c t+\varphi_l^k)} \\ &\quad + \sin\gamma_{\mathrm{ER}}^k\cos\gamma_x^k e^{j(\eta_x^k+\pi-\eta_{\mathrm{ER}}^k)}A_l^k e^{j(w_c t+\varphi_l^k)}.\end{aligned} \tag{26}$$

Then, we analyze the security performance in two special conditions:

1. For I_x and I_l, we use the constant modulus modulation technique like PSK, and we also assume their modulation order are the same. Then, $A_x^k = A_l^k$, we can derive

$$\gamma_{\mathrm{ER}}^k = \arctan\left(\frac{\left|\sin\left(\gamma_x^k\right) e^{j\varphi_x^k} - \cos\left(\gamma_x^k\right) e^{j\varphi_l^k}\right|}{\left|\cos\left(\gamma_x^k\right) e^{j\varphi_x^k} + \sin\left(\gamma_x^k\right) e^{j\varphi_l^k}\right|}\right),$$
$$\eta_{\mathrm{ER}}^k = \eta_x^k + \Xi\left(\sin\left(\gamma_x^k\right) e^{j\varphi_x^k} - \cos\left(\gamma_x^k\right) e^{j\varphi_l^k}\right) - \Xi\left(\cos\left(\gamma_x^k\right) e^{j\varphi_x^k} + \sin\left(\gamma_x^k\right) e^{j\varphi_l^k}\right). \quad (27)$$

Under this condition, both γ_{ER}^k and η_{ER}^k vary randomly. According to Eq. (26), $\mathbf{y}_{\mathrm{E}}^k(t)$ is a random complex number, therefore, the blind signal demodulation method does not work.

2. For I_x and I_l, we use the amplitude modulation technique like PAM, and we also assume their modulation order are the same. Then $\phi_x^k = \phi_l^k = 0$, the below can be derived:

$$\gamma_{\mathrm{ER}}^k = \arctan\left(\frac{\left|A_x^k \sin\left(\gamma_x^k\right) e^{j\eta_x^k} - A_l^k \cos\left(\gamma_x^k\right) e^{j\eta_x^k}\right|}{\left|A_x^k \cos\left(\gamma_x^k\right) + A_l^k \sin\left(\gamma_x^k\right)\right|}\right),$$
$$\eta_{\mathrm{ER}}^k = \Xi\left(A_x^k \sin\left(\gamma_x^k\right) e^{j\eta_x^k} - A_l^k \cos\left(\gamma_x^k\right) e^{j\eta_x^k}\right) - \Xi\left(A_x^k \cos\left(\gamma_x^k\right) + A_l^k \sin\left(\gamma_x^k\right)\right) = \eta_x^k. \quad (28)$$

Then, the received signal can be written as

$$\mathbf{y_R}(t) = \left(\cos\gamma_{\mathrm{ER}}^k \cos\gamma_x^k + \sin\gamma_{\mathrm{ER}}^k \sin\gamma_x^k\right) A_x^k e^{jw_c t} + \left(\cos\gamma_{\mathrm{ER}}^k \sin\gamma_x^k - \sin\gamma_{\mathrm{ER}}^k \cos\gamma_x^k\right) A_l^k e^{jw_c t}. \quad (29)$$

Similarly, the blind signal demodulation does not work either. Although η_x^k can be gotten, it makes little sense for the information is conveyed by the amplitude of both two polarized signals. In addition, it is also impossible for Eve to separate the two signals by PF for γ_{ER}^k varies randomly.

For other modulation technique combinations, the security performance can be analyzed in the same way and the same conclusion can be obtained. So, in the PF-PHY scheme, the modulation techniques can be chosen freely, unlike the method in [18], where PSK should be avoided.

IV. NUMERICAL SIMULATION RESULTS

In our simulations, two modulated signals are represented by $\mathbf{s}_x$ and $\mathbf{s}_l$. The transmitter designed for Alice and the receiver designed for Bob are respectively presented in Fig. 4 and Fig. 7, respectively. In addition, we only consider the case that the information about the modulation techniques applied in $\mathbf{s}_x$ and $\mathbf{s}_l$ are open to the eavesdropper Eve. This is because the case we considered is a worse one, if Eve can not demodulate the signals with these information, he can not either without these information. As Eve can not obtain the PSs of two signals, in order to demodulate the signals, blind signal demodulation method is adopted and the result after polarization match is used to recover both two signals.

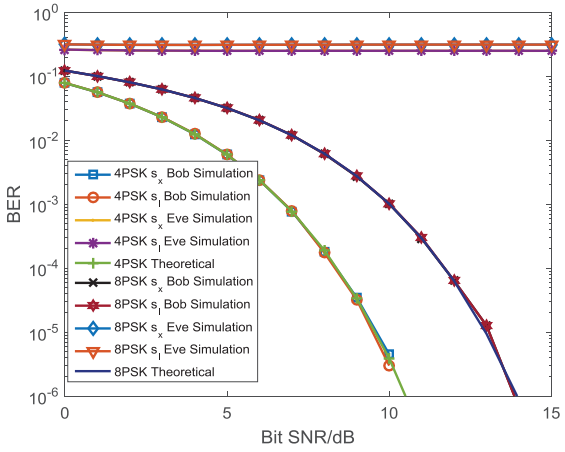

FIGURE 8. BER versus Bit SNR of 4PSK for $\mathbf{s}_x$ and $\mathbf{s}_l$ and 8PSK for $\mathbf{s}_x$ and $\mathbf{s}_l$ ($PDL = 0$ dB).

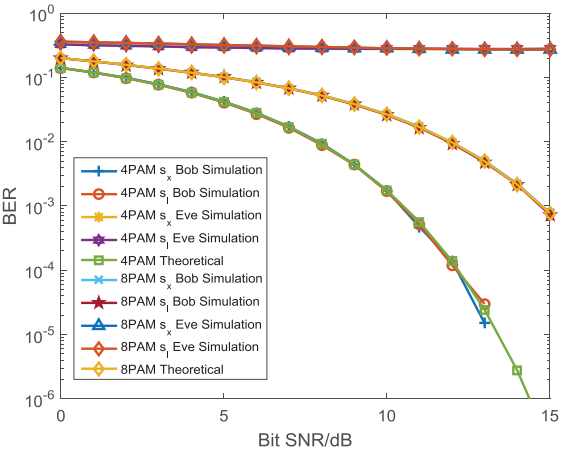

FIGURE 9. BER versus Bit SNR of 4PAM for $\mathbf{s}_x$ and $\mathbf{s}_l$ and 8PAM for $\mathbf{s}_x$ and $\mathbf{s}_l$ ($PDL = 0$ dB).

A. SECURITY PERFORMANCE WITH DIFFERENT MODULATION TECHNIQUES UNDER IDEAL GAUSS CHANNEL

To evaluate the performance of the PF-PHY scheme, an ideal Gauss channel is assumed, thus there is no PDL effect. At first, a random bit sequence is generated and divided into two parts I_x and I_l. Subsequently, different modulation techniques are utilized to modulate the two bit sequences. The PSs are selected as described in III-*C*. The BER curves are shown in Fig. 8-Fig. 11.

4PSK is firstly utilized to modulate both I_x and I_l, which results in $\mathbf{s}_x$ and $\mathbf{s}_l$. Then, their BER curves at Bob and Eve are respectively plotted. After that, we change the modulation order and utilize 8PSK to perform the same operation. The BER curves versus the bit SNR are shown in Fig. 8, it is found that the BERs of both $\mathbf{s}_x$ and $\mathbf{s}_l$ at Bob are almost the same as the theoretical values under the Gauss channel. This is because $\mathbf{s}_x$ and $\mathbf{s}_l$ are completely separated by PF at Bob. And based on the PS selection method, the noise is not amplified.

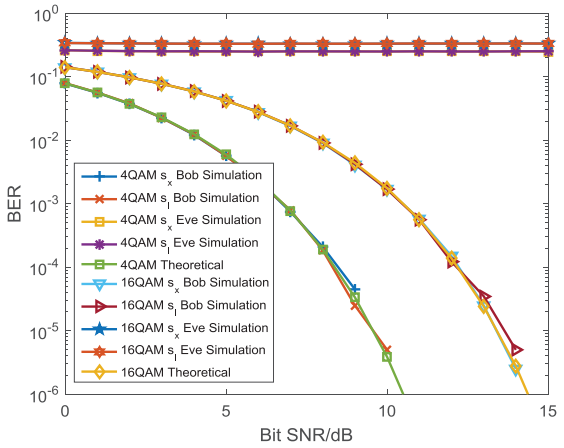

FIGURE 10. BER versus Bit SNR of 4QAM for $\mathbf{s}_x$ and $\mathbf{s}_I$ and 16QAM for $\mathbf{s}_x$ and $\mathbf{s}_I$ ($PDL = 0$ dB).

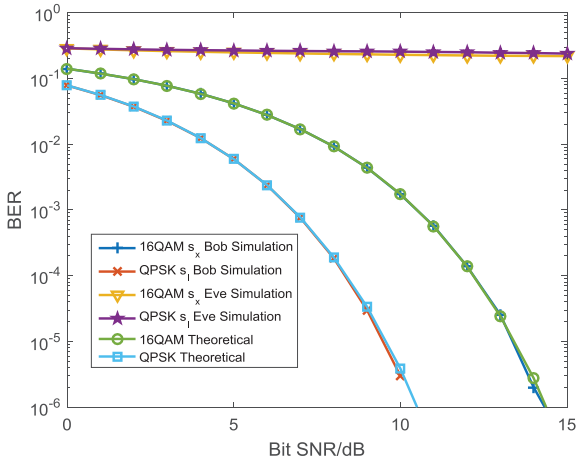

FIGURE 11. BER versus Bit SNR of 16QAM for $\mathbf{s}_x$ and QPSK for $\mathbf{s}_I$ ($PDL = 0$ dB).

However, Eve exhibits high BERs for both two signals at arbitrary SNR and modulation order.

In Fig. 9 and Fig. 10, PSK is replaced with PAM and QAM, respectively. Then, the same operations are performed. In Fig. 11, we utilize different modulation techniques to modulate I_x and I_I (16QAM for I_x and QPSK for I_I). In all these conditions, the similar results can be obtained that the BER curves of $\mathbf{s}_x$ and $\mathbf{s}_I$ at Bob are almost the same as the theoretical values, while Eve exhibits high BERs. Therefore, based on the PF-PHY scheme, Eve can hardly extract any useful information, thus the security can be enhanced.

B. SECURITY PERFORMANCE COMPARISON WITH THE FDPH METHOD IN [18]

In the FDPH method, two PSs for the k-th signal can be denoted as $\mathbf{P}_S^k\left(\gamma_S^k, \eta_S^k\right)$ and $\mathbf{P}_J^k : \left(\gamma_J^k, \eta_J^k\right) = \left(\frac{\pi}{2} - \gamma_S^k, \eta_S^k\right)$. Hence, the received signal can be represented as

$$\mathbf{y}_k(t) = \begin{bmatrix} \cos\gamma_S^k + \cos(\frac{\pi}{2} - \gamma_S^k) \\ \left(\sin\gamma_S^k + \sin(\frac{\pi}{2} - \gamma_S^k)\right) e^{j\eta_S^k} \end{bmatrix} A_O^k e^{j\left(w_c t + \varphi_O^k\right)} + \mathbf{n}, \tag{30}$$

where $\gamma_S^k \in \left[0, \frac{\pi}{8}\right]$ is the same interval as the parameter setting in [18]. For the eavesdropper Eve, the blind demodulated polarization parameters are $\left(\frac{\pi}{4}, \eta_S^k\right)$, after the polarization match is performed, the output signals can be denoted as

$$\mathbf{y}_k(t) = \sqrt{2}\left(\cos\left(\gamma_S^k\right) + \sin(\gamma_S^k)\right) A_O^k e^{j\left(w_c t + \varphi_O^k\right)} + \mathbf{n}. \tag{31}$$

From Eq. (31), It can be found that the amplitude varies randomly due to the fast hopping PS, while the phase does not change. Therefore, the modulation techniques like PSK are not applicable. In addition, we find that once PSK is used, the power of the signal is amplified due to

$$\sqrt{2}\left(\cos\left(\gamma_S^k\right) + \sin(\gamma_S^k)\right) \geq \sqrt{2}. \tag{32}$$

The simulation results are shown in Fig. 12, it can be found that the BER of Bob in PF-PHY is almost the same as the theoretical values, while the BER of Bob in FDPH is a little worse, this is because the principle angle ξ is smaller than $\frac{\pi}{2}$, which amplifies the noise power as shown in Fig. 5. In addition, the BER of Eve in PF-PHY is higher, while BER of Eve in FDPH is better than the theoretical values. This is because after performing the polarization match, the signal power is amplified as shown in Eq. (32). This is the different result we obtained from the result in [18].

When using other modulations, for Bob, we can obtain the similar results that the BER performance of the PF-PHY scheme outperforms that of the FDPH scheme.

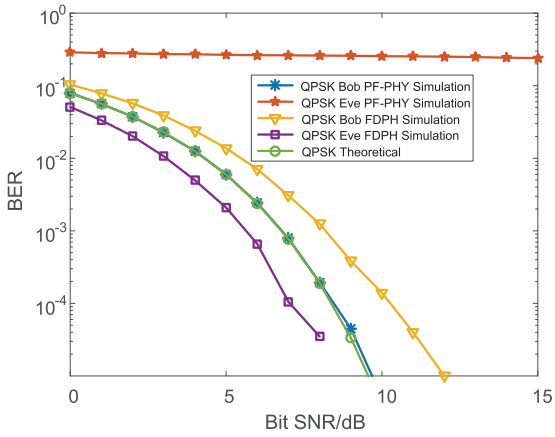

FIGURE 12. BER performance comparison of FDPH and PF-PHY ($PDL = 0$ dB).

C. PDL ELIMINATION PERFORMANCE WITH NON-IDEAL GAUSS CHANNEL

This simulation tries to to compare the PDL elimination performance of the ZFPF method and the PC method. The statistical modeling of land mobile satellite channels [5] is utilized and the BER curves for Bob are plotted in Fig. 13, where $PDL = 3$ dB. Two modulation techniques (QPSK and 8PSK) are used to modulate I_x and I_I, respectively. From Fig. 13, it can be found that the BER performance of ZFPF is a little better than that of PC and both of them are a little worse than the theoretical values. This is because in the ZFPF method, the noise power is amplified and in the

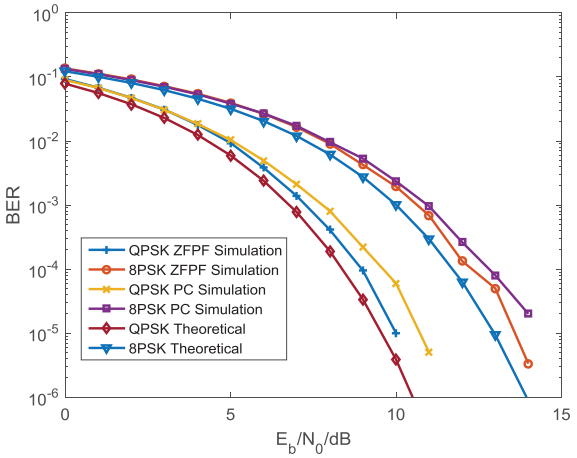

FIGURE 13. PDL elimination performance comparison (*PDL* = 3 dB).

PC method, the signal's power decreases after being processed by the pre-compensation matrix. In addition, with the usage of the ZFPF method, we just have to calculate the channel matrix during every channel estimation interval, while if the PC method is utilized, the pre-compensation matrix should be updated at the symbol rate, which accounts more calculations. Furthermore, in the ZFPF method, CSI is estimated at the receiver side, which is more practical in satellite scenarios.

V. CONCLUSION

This paper puts forward a polarization filtering based transmission scheme to enhance the physical layer security in the dual-polarized satellite communication. The information sequence is transmitted by two different polarized signals at the same time, which has a higher transmission efficiency than the FDPH method. In the PF-PHY scheme, constant modulus modulation technique can be directly used to modulate the signals, while for FDPH, PSK only can be used with the time-varying channel. Finally, to eliminate the PDL effect, the ZFPF method is utilized, which requires less computation than the PC method and is more practical in satellite scenarios.

REFERENCES

[1] E. G. Larsson, O. Edfors, F. Tufvesson, and T. L. Marzetta, "Massive MIMO for next generation wireless systems," *IEEE Commun. Mag.*, vol. 52, no. 2, pp. 186–195, Feb. 2014.
[2] L. Lu, G. Y. Li, A. L. Swindlehurst, A. Ashikhmin, and R. Zhang, "An overview of massive MIMO: Benefits and challenges," *IEEE J. Sel. Topics Signal Process.*, vol. 8, no. 5, pp. 742–758, Oct. 2014.
[3] Z. Luo, H. Wang, and W. Lv, "Pilot contamination mitigation via a novel time-shift pilot scheme in large-scale multicell multiuser MIMO systems," *Int. J. Antennas Propag.*, vol. 2016, Sep. 2016, Art. no. 7628692.
[4] J. Arnau and C. Mosquera, "Dissection of multibeam satellite communications with a large-scale antenna system toolbox," in *Proc. 20th Eur. Wireless Conf.*, Barcelona, Spain, May 2014, pp. 1–6.
[5] K. P. Liolis, J. Gomez-Vilardebo, E. Casini, and A. I. Perez-Neira, "Statistical modeling of dual-polarized MIMO land mobile satellite channels," *IEEE Trans. Commun.*, vol. 58, no. 11, pp. 3077–3083, Nov. 2010.
[6] C. Guo, X. Wu, C. Feng, and Z. Zeng, "Spectrum sensing for cognitive radios based on directional statistics of polarization vectors," *IEEE J. Sel. Areas Commun.*, vol. 31, no. 3, pp. 379–393, Mar. 2013.
[7] P. Arapoglou, P. Burzigotti, M. Bertinelli, A. B. Alamanac, and R. De Gaudenzi, "To MIMO or not to MIMO in mobile satellite broadcasting systems," *IEEE Trans. Wireless Commun.*, vol. 10, no. 9, pp. 2807–2811, Sep. 2011.
[8] D. Wei, C. Feng, C. Guo, and L. Fangfang, "A power amplifier energy efficient polarization modulation scheme based on the optimal pre-compensation," *IEEE Commun. Lett.*, vol. 17, no. 3, pp. 513–516, Mar. 2013.
[9] L. Arend, R. Sperber, M. Marso, and J. Krause, "Implementing polarization shift keying over satellite—System design and measurement results," *Int. J. Satellite Commun. Netw.*, vol. 34, no. 2, pp. 211–229, May 2015.
[10] B. Cao, Q.-Y. Zhang, and L. Jin, "Polarization division multiple access with polarization modulation for los wireless communications," *EURASIP J. Wireless Commun. Netw.*, vol. 2011, p. 77, Dec. 2011.
[11] N. Mazzali, F. Kayhan, and R. B. S. Mysore, "Four-dimensional constellations for dual-polarized satellite communications," in *Proc. IEEE Int. Conf. Commun.*, Kuala Lumpur, Malaysia, May 2016, pp. 1–6.
[12] B. Cao, Q.-Y. Zhang, D. Liang, S.-M. Wen, L. Jin, and Y.-Q. Zhang, "Blind adaptive polarization filtering based on oblique projection," in *Proc. IEEE Int. Conf. Commun.*, Cape Town, South Africa, May 2010, pp. 1–5.
[13] G. Zheng, P.-D. Arapoglou, and B. Ottersten, "Physical layer security in multibeam satellite systems," *IEEE Trans. Wireless Commun.*, vol. 11, no. 2, pp. 852–863, Feb. 2012.
[14] D. Shan, K. Zeng, W. Xiang, P. Richardson, and Y. Dong, "PHY-CRAM: Physical layer challenge-response authentication mechanism for wireless networks," *IEEE J. Sel. Areas Commun.*, vol. 31, no. 9, pp. 1817–1827, Sep. 2013.
[15] W. Trappe, "The challenges facing physical layer security," *IEEE Commun. Mag.*, vol. 53, no. 6, pp. 16–20, Jun. 2015.
[16] J. Lei, H. Zhu, M. Á. Vazquez-Castro, and A. Hjorungnes, "Secure satellite communication systems design with individual secrecy rate constraints," *IEEE Trans. Inf. Forensics Security*, vol. 6, no. 3, pp. 661–671, Sep. 2011.
[17] Z. Luo, H. Wang, and K. Zhou, "Physical layer security scheme based on polarization modulation and wfrft processing for dual-polarized satellite systems," *KSII Trans. Internet Inf.*, to be published.
[18] X. Zhang, B. Zhang, and D. Guo, "Physical layer secure transmission based on fast dual polarization hopping in fixed satellite communication," *IEEE Access*, vol. 5, pp. 11782–11790, Jun. 2017.
[19] Z. Wen, F. Chunyan, L. Fangfang, and G. Caili, "Polarization oblique projection based self-interference cancellation against PA nonlinear distortion in MIMO full duplex system," *China Commun.*, vol. 13, no. 11, pp. 49–59, Nov. 2016.
[20] W. Dong, Z. Meng, F. Wei, and H. Weiqing, "A spectrum efficient polarized PSK/QAM scheme in the wireless channel with polarization dependent loss effect," in *Proc. IEEE Int. Conf. Telecommun.*, Sydney, NSW, Australia, Apr. 2015, pp. 249–255.
[21] R. Ma, L. Dai, Z. Wang, and J. Wang, "Secure communication in TDS-OFDM system using constellation rotation and noise insertion," *IEEE Trans. Consum. Electron.*, vol. 56, no. 3, pp. 1328–1332, Aug. 2010.
[22] D. Wei, C. Feng, and C. Guo, "An optimal pre-compensation based joint polarization-amplitude-phase modulation scheme for the power amplifier energy efficiency improvement," in *Proc. IEEE Int. Conf. Commun. (ICC)*, Jun. 2013, pp. 4137–4142.
[23] P. Henarejos and A. Pérez-Neira, "Dual polarized modulation and reception for next generation mobile satellite communications," *IEEE Trans. Commun.*, vol. 63, no. 10, pp. 3803–3812, Oct. 2015.
[24] Y. Yang, X. Xin, J. Bin, and G. Xiqi, "An adaptive coding method for dual-polarized mobile satellite communications," in *Proc. IEEE Int. Conf. Wireless Commun. Signal Process.*, Hefei, China, Oct. 2013, pp. 1–5.

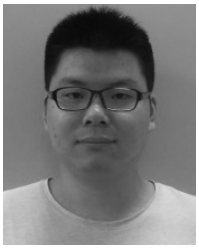

ZHANGKAI LUO received the B.Eng. degree in communication engineering from the Hebei University of Technology, Tianjin, China, in 2011. He is currently pursuing the Ph.D. degree with PLA Army Engineering University, China. His research interests include satellite communication and signal processing.

HUALI WANG received the Ph.D. degree in electronic engineering from the Nanjing University of Science and Technology, China, in 1997. He is currently a Professor with the Nanjing College of Communication Engineering, PLA Army Engineering University, China. His research interests include satellite communication and signal processing.

KAIJIE ZHOU received the B.Eng. degree in electrical engineering and automation from the Hefei University of Technology, Hefei, China, in 2007. He is currently pursuing the Ph.D. degree with PLA Army Engineering University, China. His research interests include satellite communication and signal processing.